The Chemical Evolution of Protoplanetary Disks

Edwin A. Bergin
University of Michigan

Yuri Aikawa
Kobe University

Geoffrey A. Blake
California Institute of Technology

Ewine F. van Dishoeck
Leiden Observatory

In this review we re-evaluate our observational and theoretical understanding of the chemical evolution of protoplanetary disks. We discuss how improved observational capabilities have enabled the detection of numerous molecules exposing an active disk chemistry that appears to be in disequilibrium. We outline the primary facets of static and dynamical theoretical chemical models. Such models have demonstrated that the observed disk chemistry arises from warm surface layers that are irradiated by X-ray and FUV emission from the central accreting star. Key emphasis is placed on reviewing areas where disk chemistry and physics are linked: including the deuterium chemistry, gas temperature structure, disk viscous evolution (mixing), ionization fraction, and the beginnings of planet formation.

1. INTRODUCTION

For decades models of our own Solar nebular chemical and physical evolution have been constrained by the chemical record gathered from meteorites, planetary atmospheres, and cometary comae. Such studies have provided important clues to the formation of the sun and planets, but large questions remain regarding the structure of the solar nebula, the exact timescale of planetary formation, and the chemical evolution of nebular gas and dust. Today we are on the verge of a different approach to nebular chemical studies, one where the record gained by solar system studies is combined with observations of numerous molecular lines in a multitude of extra-solar protoplanetary disk systems tracking various evolutionary stages.

Our observational understanding of extra-solar protoplanetary disk systems is still in its infancy as the current capabilities of millimeter-wave observatories are limited by sensitivity and also by the small angular size of circumstellar disks, even in the closest star-forming regions ($< 3-4''$). Nonetheless, numerous molecules have been detected in protoplanetary disks, exposing an active chemistry (*Dutrey et al.*, 1997; *Kastner et al.*, 1997; *Qi et al.*, 2003; *Thi et al.*, 2004). Since the last *Protostars & Planets* review (*Prinn*, 1993) these observations have led to a paradigm shift in our understanding of disk chemistry. For many years focus was placed on thermochemical models as predictors of the gaseous composition, and these models have relevance in the high pressure, $\gtrsim 10^{-6}$ bar, (inner) regions of the

nebula (e.g., *Fegley*, 1999). However, for most of the disk mass, the observed chemistry appears to be in disequilibrium and quite similar to that seen in dense regions of the interstellar medium (ISM) that are directly exposed to radiation (*Aikawa and Herbst, 1999*; *Willacy and Langer*, 2000; *Aikawa et al.*, 2002).

In this review we focus on gains in our understanding of the chemistry that precedes and is contemporaneous with the formation of planets from a perspective guided by observations of other stellar systems whose masses are similar to the Sun. We examine both the observational and theoretical aspects of this emerging field, with an emphasis on areas where the chemistry directly relates to disk physics. Portions of this review overlap with other chapters, such as the observational summary of molecular disks, inner disk gas, and disk physical structure (see the chapters by Dutrey et al., Najita et al., and Dullemond et al., respectively). For this purpose we focus our review on the physics and chemistry of the outer disk ($r > 10$ AU) in systems with ages of 0.3-10 Myr. In support of theory we also present an observational perspective extending from the infrared (IR) to the submillimeter (sub-mm) to motivate the theoretical background and supplement other discussions.

2. GENERAL THEORETICAL PICTURE

2.1. Basic Physical and Chemical Structure of Disk

Chemical abundances are determined by physical conditions such as density, temperature, and the incident
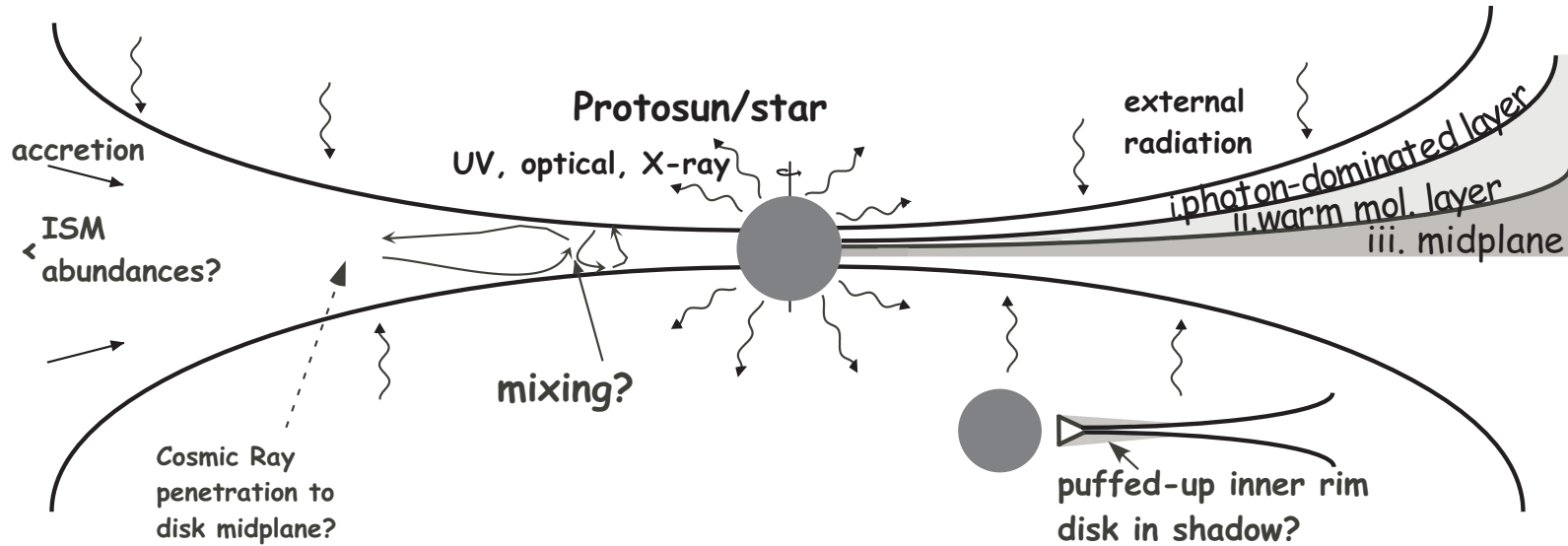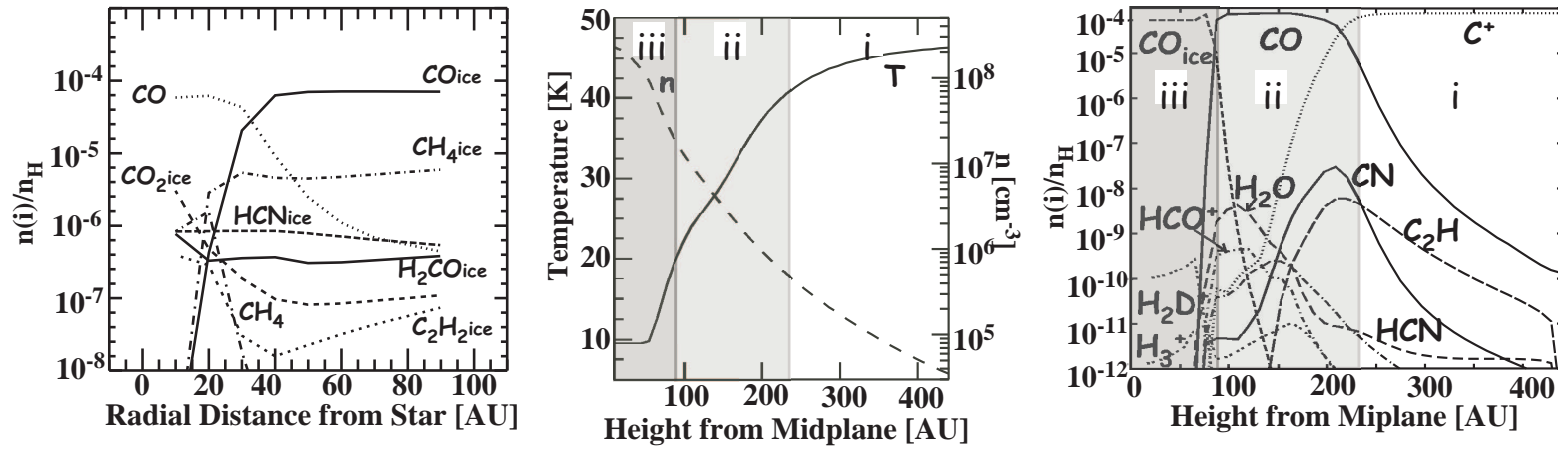
Fig. 1.— Chemical structure of protoplanetary disks. Vertically the disk is schematically divided into three zones: a photon-dominated layer, a warm molecular layer, and a midplane freeze-out layer. The CO freeze-out layer disappears at $r \lesssim 30 - 60$ AU as the mid-plane temperature increases inwards. Various non-thermal inputs, cosmic ray, UV, and X-ray drive chemical reactions. Viscous accretion and turbulence will transport the disk material both vertically and radially. The upper panels show the radial and vertical distribution of molecular abundances from a typical disk model at the midplane (*Aikawa et al.*, 1999) and $r \sim 300$ AU (*van Zadelhoff et al.*, 2003). A sample of the hydrogen density and *dust* temperature at the same distance (*D'Alessio et al.*, 1999) is also provided. In upper layers ($\gtrsim 150$ AU) the *gas* temperature will exceed the dust temperature by $\gtrsim 25$ K (*Jonkheid et al.* 2004).

radiation field. Recent years have seen significant progress in characterizing disk physical structure, which aids in understanding disk chemical processes. Isolated disks can be quite extended with $r_{out} \sim$ one hundred to a few hundred AU (*Simon et al.* 2000), much larger than expected from comparison with the Minimum Mass Solar Nebula (MMSN: *Hayashi*, 1981). Although, it should be stated that we have an observational bias towards detecting larger disks due to our observational limitations. The radial distribution of column density and midplane temperature have been estimated by observing thermal emission of dust; they are fitted by a power-law $\Sigma(r) \propto r^{-p}$ and $T(r) \propto r^{-q}$, with $p = 0 - 1$ and $q = 0.5 - 0.75$. The temperature at 1 AU is $\sim 100 - 200$ K, while the surface density at 100 AU is $0.1 - 10$ g cm^{-2} (e.g., *Beckwith et al.*, 1990; *Kitamura et al.*, 2002).

The vertical structure is estimated by calculating the hydrostatic equilibrium for the density and radiation transfer for the dust temperature (see the chapter by *Dullemond et al.*). Beyond several AU the disk is mainly heated by irradiation from the central star. The stellar radiation is absorbed by grains at the disk surface, which then emit thermal radiation to heat the disk interior (*Calvet et al.*, 1992; *Chiang and Goldreich*, 1997; *D'Alessio et al.*, 1998). Hence the temperature decreases towards the midplane, as seen in Fig. 1. For small radii ($r <$ few AU), however, heating by mass accretion is not negligible and the midplane can be warmer than the disk surface. At $r = 1$ AU, for example, the midplane temperature can be as high as 1000 K, if the accretion rate is large (*D'Alessio et al.*, 1999; *Nomura*, 2002). The density distribution is basically Gaussian, $\exp -(Z/H)^2$, with some deviation due to vertical temperature variations (see Fig. 1). As a whole the disk has a flared-up structure, with a geometrical thickness that increases with radius (*Kenyon and Hartmann*, 1987).

Based on such physical models, the current picture of the general disk chemical structure is schematically shown in Fig. 1. At $r \gtrsim 100$ AU, the disk can be divided into three layers: the photon dominated region (PDR), the warm molecular layer, and the midplane freeze-out layer. The disk is irradiated by UV radiation from the central star and interstellar radiation field that ionize and dissociate molecules and atoms in the surface layer. In the midplane the temperature is mostly lower than the freeze-out temperature of CO (~ 20 K), one of the most abundant and volatile molecules in the ISM. Since the timescale of adsorption onto grains is short at high density ($\sim 10(10^9 \text{cm}^{-3}/n_{\text{H}})$ yr), heavy-element species are significantly depleted onto grains. At intermediate heights, the temperature is several 10s of K, and the density is sufficiently high ($\gtrsim 10^6$ cm^{-3}) to ensure the existence of molecules even if the UV radiation is not completely attenuated by the upper layer (*Aikawa and Herbst*, 1999; *Willacy and Langer*, 2000; *Aikawa et al.*, 2002). Here water is still frozen onto grains, trapping much of the oxygen in the solid state. Thus, the warm CO-rich gas layers will have C/O ~ 1, leading to a rich and extensive carbon-based chemistry.

These models provide a good match to observed abundances. *Dutrey et al.* (1997) found that in the DM Tau disk, molecular abundances are generally lower than in dense clouds, but the CN/HCN ratio is higher (see also *Thi et al.*, 2004). The low molecular abundances are caused by depletion in the midplane, and the high CN/HCN ratio originates in the surface PDR (cf. Fig. 1), as seen in PDRs in the ISM (*Rodríguez-Franco et al.*, 1998).

At $r \lesssim 100$ AU, the midplane temperature is high enough to sublimate various ice materials that formed originally in the outer disk radius and/or parental cloud core (e.g., *Markwick et al.*, 2002). This sublimation will be species dependent with the "snow line" for a given species appearing at different radii. For example, in the solar nebula the water ice snow line appeared near 3–5 AU, while the CO snow line would appear at greater distances where the midplane dust temperatures drop below ~ 20 K. Within these species-selective gaseous zones, sublimated molecules will be destroyed and transformed to other molecules by gas-phase reactions. In this fashion, the chemistry is similar to the so-called "hot core" chemistry, which appears in star-forming cores surrounding protostars (e.g., *Hatchell et al.*, 1998; see the chapter by *Ceccarelli et al.*). For example, sublimated CH$_4$ is transformed to larger and less volatile carbon-chain species, which can then accumulate onto grains (*Aikawa et al.*, 1999).

2.2. Key Ingredients: UV, X-ray, and Cosmic-ray

Thermochemistry and its consequences are described by *Fegley et al.* (1989) and *Prinn et al.* (1993). In recent years non-thermal events such as cosmic rays, UV and X-rays have been included in the disk chemistry models and shown to play important roles.

In molecular clouds, chemical reactions are driven by cosmic-ray ionization (e.g., *Herbst and Klemperer*, 1973). Since cosmic-ray ionization has an attenuation length of 96 g cm^{-2} (*Umebayashi and Nakano*, 1981), in the disk it can be important, for $r \gtrsim$ several AU, in driving ion-molecule reactions and producing radicals which undergo neutral-neutral reactions (*Aikawa et al.*, 1997). Although cosmic rays may be scattered by the magnetic fields within and around the protostar-disk system, detection of ions (e.g., HCO$^+$ and H$_2$D$^+$) and comparison with theoretical models indicate that some ionization mechanisms, perhaps cosmic-rays, is available at least for $r \gtrsim 100$ AU (*Semenov et. al.* 2004; *Ceccarelli and Dominik* 2005) (see also § 4.3).

T Tauri stars have excess UV flux that is much higher than expected from their effective temperature of ~ 3000 K (e.g., *Herbig and Goodrich*, 1986). It is considered to originate in the accretion shock on the stellar surface (*Calvet and Gullbring*, 1998), with potential contributions from an active chromosphere (*Alexander et al.*, 2005). For low-mass T Tauri stars, the strength of the UV field is often parameterized in terms of the local interstellar radiation field (*Habing*, 1968; $G_0 = 1$), and have values of $G_0 \sim 300 - 1000$ at 100 AU (*Bergin et al.*, 2004). This radiation impinges on
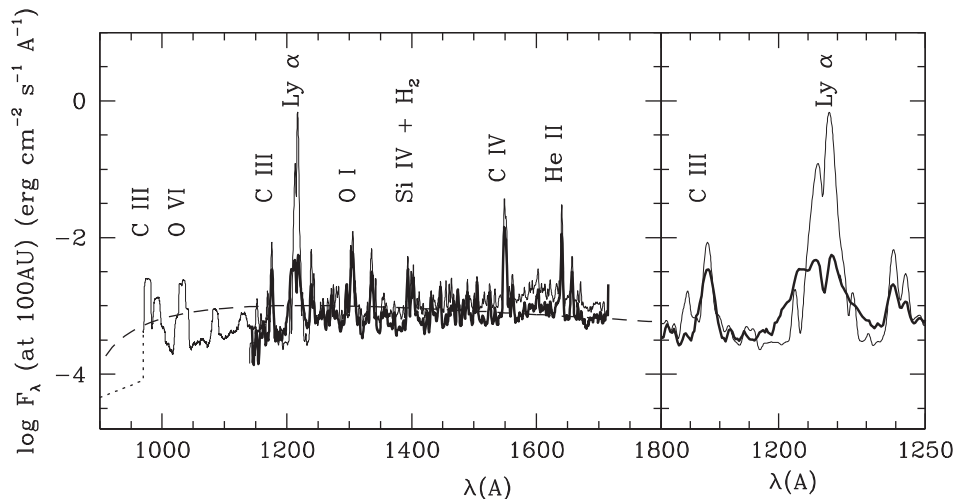
Fig. 2.— UV spectra of T Tauri stars. Heavy solid lines and light solid lines represent the spectra of BP Tau and TW Hya, respectively. The spectrum of TW Hya is scaled by 3.5 to match the BP Tau continuum level. The long dashed line represents the interstellar radiation field of *Draine* (1978) scaled by a factor of 540. The region around the Lyα line is enlarged in the right panel. Taken from *Bergin et al.* (2003).

the flared disk surface with a shallow angle of incidence. Stellar and interstellar UV photons dissociate and ionize molecules and atoms in the flared disk surfaces and detailed two-dimensional radiative transfer models are required to quantitatively predict molecular abundances. *van Zadelhoff et al.* (2003) showed scattering of stellar UV at the disk surface significantly enhances the abundance of radical species in deeper layers, and examined the resulting chemical evolution for different wavelength dependencies of the stellar UV radiation field. *Bergin et al.* (2003) pointed out the importance of Ly α emission, which stands out in the UV spectrum of T Tauri stars (Fig. 2) and is absent from the interstellar field. In the one case where the line is unaffected by interstellar absorption, TW Hya, Ly α radiation carries $\sim 85\%$ of the FUV flux (*Herczeg et al.* 2004). Since photodissociation cross sections are a function of wavelength, species that absorb Lyman α, such as HCN and H_2O, will be selectively dissociated, while others, such as CO and H_2, are unaffected (*van Dishoeck et al.*, 2006).

Most stars do not form in isolation, rather 70-90% stars are born in GMC's (which contain most of the Galactic molecular mass) and are found in embedded stellar clusters (*Lada and Lada* 2003). In this light there exists growing evidence that the Sun formed in a cluster in the vicinity of a massive star (see the chapter by *Wadhwa et al.*; *Hester and Desch* 2006). In this case the UV radiation field can be much higher, depending on the spectral type of the OB star, the proximity of the low mass star to the source of energetic radiation, and on the dissipation timescale of the surrounding dust and gas (which can shield forming low mass disks from radiation). After gas/dust dissipation the external radiation has greater penetrating power, because it can impinge on the disk with a greater angle of incidence. The primary effects of external radiation, if it dominates the stellar contribution, will be to magnify the chemistry (e.g., CO driven

photo-chemistry) produced by the stellar radiation and increase the size of the warm molecular layer.

Strong X-ray emission is observed toward T Tauri stars (e.g., *Kastner et al.*, 2005). It may originate in the magnetic reconnections either in the stellar magnetosphere, at the star-disk interface, or above the circumstellar disk (*Feigelson and Montmerle*, 1999 and references therein). X-rays affect the chemistry in several ways (*Maloney et al.*, 1996; *Stäuber et al.*, 2005). (1) They ionize atoms and molecules to produce high-energy photoelectrons that further ionize the gas. On the disk surface X-ray ionization produces a higher ionization rate than cosmic-rays, and can even be the dominant ionization source if the cosmic-rays are scattered by the magnetic field (*Glassgold et al.*, 1997; *Igea and Glassgold*, 1999). (2) High-energy photoelectrons heat the gas. For example, at $r = 1$ AU, the gas temperature in the upper most layer can be as high as 5000 K due to the X-ray heating together with mechanical heating such as turbulent dissipation (*Glassgold et al.*, 2004; see the chapter by *Najita et al.*). (3) Collision of the high-energy electrons with hydrogen atoms and molecules results in excitation of these species and then the emission of UV photons within the disk (*Maloney et al.*, 1996; *Herczeg et al.*, 2004). Recently *Bergin et al.* (2004) found H_2 FUV continuum emission caused by this mechanism. The high ionization rate and induced photodissociation of CO enhance the abundances of organic species such as CN, HCN. and HCO^+ (*Aikawa and Herbst*, 1999; 2001).

Non-thermal particles and radiation can also drive the desorption of molecular species from the grain surface. Because of the high densities, gaseous species collide with grains on short timescales. In the low-temperature region in the outer disk the colliding molecules are adsorbed onto grains, and thermal desorption is inefficient except for very volatile species such as CO, N_2, and CH_4, depending on the

4

temperature. Various gaseous molecules are still observable since they are formed from CO and N_2 via gas-phase reactions, that compensates for adsorption (e.g., *Aikawa et al.* 2002). However, observations may indicate the need more efficient (thermal or non-thermal) desorption, especially for species mainly formed by grain-surface reactions. For example, *Dartois et al.* (2003) find evidence for gaseous CO in layers with a temperature below the CO sublimation temperature. Cosmic-rays and X-rays can temporally 'spot heat' the grains to enhance desorption rates (e.g., *Léger et al.*, 1985; *Hasegawa and Herbst*, 1993). UV radiation can also desorb molecules, possibly by producing radicals within the ice mantle, which react with other radicals on the grain surface to release excess energies (*Westley et al.*, 1995). It should be noted, however, that the non-thermal desorption rates are uncertain and depend on various parameters such as structure of the grain particle (*Najita et al.*, 2001), UV flux, number density of radical species in grain mantle (*Shen et al.*, 2004), and detailed desorption process (*Bringa and Johnson*, 2004). Mixing could also play a role in moving material from warmer layers to colder ones (e.g., Section 4.4).

3. Observations

Observational studies of the chemistry in extrasolar protoplanetary disks started only in the last decade thanks to improved sensitivity and spatial resolution at millimeter and IR wavelengths. At millimeter wavelengths, molecules other than CO have now been detected and imaged in a handful of disks with single-dish telescopes and interferometers. This technique has the advantage that molecules with very low abundances (down to 10^{-11} with respect to H_2) can be detected through their pure rotational transitions, and that the spatial distribution in the disk can be determined. With a spectral resolving power $R \approx \lambda/\Delta\lambda > 10^6$, the line profiles are fully resolved and kinematic information can be derived. Infrared spectroscopy has the main advantage that not only gas but also solid material can be probed through their vibrational transitions, including ices and silicates. Also, gas-phase molecules without dipole moments, including H_2, CH_4, C_2H_2 and CO_2, can only be observed at IR wavelengths. Finally, Polycyclic Aromatic Hydrocarbons (PAHs) have unique IR features. For space-based instruments, the resolving power is usually low, typically $R \approx 300 - 3000$, making it difficult to observe and resolve gas-phase lines.

3.1. Infrared observations

3.1.1. Silicates, ices and PAHs. The *Infrared Space Observatory* (ISO) opened up mid-IR spectroscopy of disks over the full 2–200 μm range unhindered by the Earth's atmosphere, revealing a wealth of features (see *van Dishoeck*, 2004 for a review). Because of limited sensitivity, ISO could only probe the chemistry in disks around intermediate-mass Herbig Ae/Be stars. The *Spitzer Space Telescope* has the sensitivity to take 5–40 μm spectra of

solar-mass T Tauri stars, while large 8–10m optical telescopes can obtain higher spectral and spatial resolution data in atmospheric windows, most notably at 3–4, 4.6–5 and 8–13 μm. The features are usually in emission, except if the disk is viewed nearly edge-on when the bands occur in absorption against the continuum of the warm dust in the inner disk.

The amorphous broad silicate features at ~10 and 20 μm are the most prominent emission bands in disk spectra (e.g., *Przygodda et al.* 2003, *Kessler-Silacci et al.* 2005; 2006) (see Fig. 3). They arise in the super-heated layers of the inner disk at <1–10 AU and are not representative of the outer disk. For at least half of the sources narrower features are seen as well, which can be ascribed to crystalline silicates such as forsterite, Mg_2SiO_4 (e.g., *Malfait et al.*, 1998, *Forrest et al.*, 2004). Silicates are discussed extensively in the chapter by *Natta et al.*, the main point for this chapter is that the shape and strength of the silicate features, together with the overall spectral energy distribution, can be used to determine whether grain growth and settling has occurred (e.g., *van Boekel et al.*, 2005). This, in turn, affects the chemistry and heating in the disk (see Section 4.1). Also, the presence of crystalline silicates may be an indication of significant radial and vertical mixing (see Section 4.4).

Ices can only be present in the cold, outer parts of the disk where the temperature drops below 100 K. Thus, the strongest ice emission bands typically occur at far-IR wavelengths. Crystalline water ice has been seen in a few disks through librational features at 44 and 63 μm (e.g., *Malfait et al.*, 1998, *Chiang et al.*, 2001). The data can be reproduced in models assuming that 50% of the available oxygen is in water ice. Edge-on disks offer a special opportunity to study ices at mid-IR wavelengths in absorption. Examples are L1489 (*Boogert et al.* 2002), DG Tau B (*Watson et al.* 2004) and CRBR2422.8-3423 (*Thi et al.* 2002, *Pontoppidan et al.* 2005)(Fig. 3). Extreme care has to be taken in the interpretation of these data since a large fraction of the ice features may arise in foreground clouds. For the case of CRBR 2422.8-3423, a disk viewed at an inclination of ~70°, comparison with nearby lines of sight through the same core combined with detailed disk modeling has been used to constrain the amount of ice in the disk. H_2O ice has an average line-of-sight abundance of ~ 10^{-4} relative to H_2, consistent with significant freeze-out. CO_2 and CO ice are also present, the latter only in the form where it is mixed with H_2O ice. The shape of the 6.85 μm ice band –usually ascribed to NH_4^+ (e.g., *Schutte and Khanna*, 2004)– shows evidence for heating to 40–50 K, as expected in the warm intermediate layers of the disk. Future studies of a large sample of edge-on disks can provide significant insight into the abundance and distribution of ices in disks, because the ice absorption depths, band shapes and feature ratios depend strongly on the disk temperature structure and line of sight, i.e., inclination (*Pontoppidan et al.*, 2005).

PAHs are important in the chemistry for at least three reasons: as absorbers of UV radiation, as a heating agent for the gas, and as potential sites of H_2 formation when
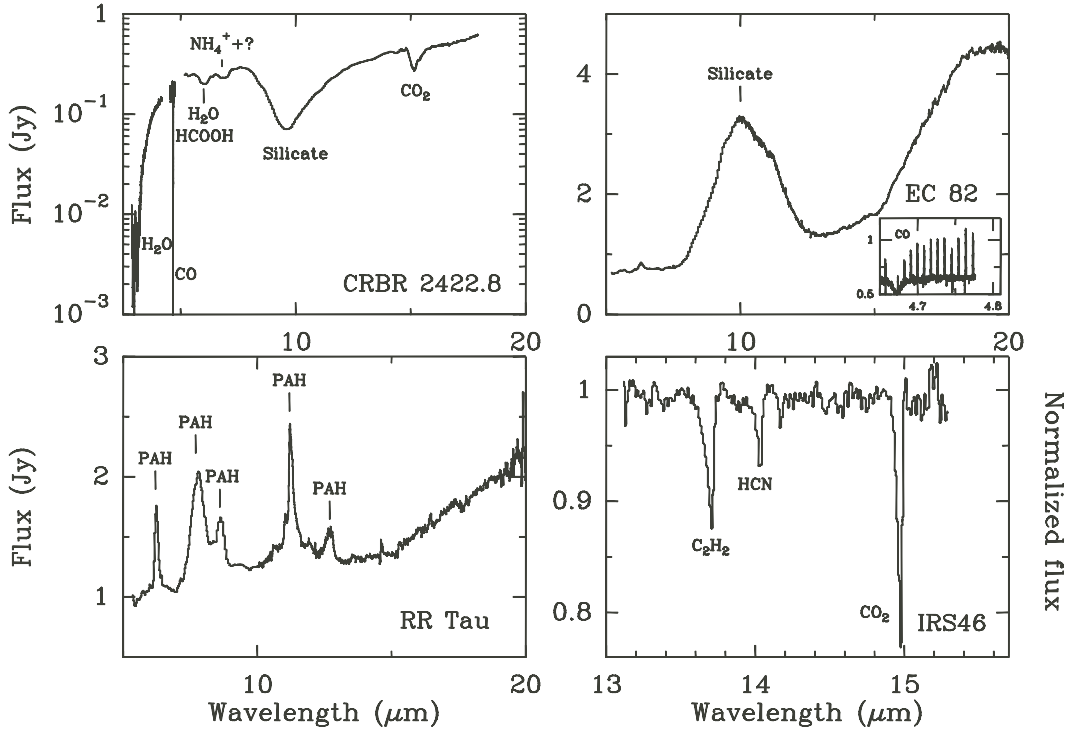
Fig. 3.— *Top left:* ice features toward edge-on disk CRBR 2422.8 -3423. Some absorptions arise in the cold foreground core (*Pontoppidan et al.*, 2005). *Top right:* silicate emission at 10 and 20 μm toward EC 82 (*Kessler-Silacci et al.*, 2006); inset, gas-phase CO v=1-0 emission (*Blake and Boogert*, priv. comm.). *Bottom right:* PAH features toward RR Tau (*Geers et al.*, 2006, in prep.); *Bottom left:* gaseous C_2H_2, HCN and CO_2 toward IRS 46 in Oph (*Lahuis et al.*, 2006);

classical grains have grown to large sizes. Since they require UV radiation for excitation, PAHs are also excellent diagnostics of the stellar radiation field and disk shape (flaring or flat). PAHs are detected in the spectra of at least 50% of Herbig Ae stars with disks through emission features at 3.3, 6.2, 7.7, 8.6, 11.2, 12.8 μm (*Acke and van den Ancker* 2004). For T Tauri stars, the features are weaker and more difficult to see on top of the strong continuum, but at least 8% of sources with spectral types later than F7 show the 11.2 μm PAH feature (*Geers et al. 2006*, in prep.). Ground-based long-slit spectroscopy and narrow-band imaging at sub-arcsec resolution has demonstrated that, at least for some disks, the PAH emission comes from a region of radius 10–100 AU (e.g., *Geers et al.*, 2004, *Habart et al.*, 2004). The inferred PAH abundance is typically 10^{-7} with respect to H_2, assuming that $\sim$10% of the carbon is in PAHs with 50-100 carbon atoms. PAHs have been detected in transitional disks, where there is evidence for grain growth to μm size, albeit at a low abundance of 10^{-9} (*Li and Lunine*, 2003, *Jonkheid et al.*, 2006). This indicates that the PAHs and very small grains in the upper disk layer may be decoupled dynamically from the larger silicate grains and have a much longer lifetime toward grain growth and settling.

Gas-phase molecules. Vibration-rotation emission lines of gaseous CO at 4.7 μm are detected toward a large fraction (>80%) of T Tauri and Herbig Ae stars with disks (e.g.,

Najita et al., 2003, *Brittain and Rettig*, 2002, *Blake and Boogert*, 2004). The CO lines can be excited by collisions in the hot gas in the inner (<5–10 AU) disk as well as by IR or UV pumping in the upper layers of the outer ($r > 10$ AU) disk. Searches for other molecular emission lines have so far been largely unsuccessful except for the detection of hot H_2O toward one young star, presumably arising in the inner disk (*Carr et al.*, 2004). A tentative detection of H_3^+ – a potential tracer of protoplanets – has been claimed toward one young star (HD141569; *Brittain and Rettig*, 2002), but this remains unconfirmed (*Goto et al.*, 2005).

Surprisingly, *Spitzer* has recently detected strong absorption from C_2H_2, HCN, and CO_2 at $R = 600$ toward one young star with an edge-on disk, IRS 46 in Ophiuchus (Fig. 3) (*Lahuis et al.* 2006). The inferred abundances are high, $\sim 10^{-5}$ with respect to H_2, and the gas is hot, 300–700 K, with linewidths of $\sim$ 20 km s^{-1}. The most likely location for this hot gas rich in organic molecules is in the inner (<few AU) disk, with the line of sight passing through the puffed-up inner rim. The observed abundances are comparable to those found in inner disk chemistry models (e.g., *Markwick et al.* 2002).

A novel method to probe the chemistry in the outer ($r > 10$ AU) disk is through observations of narrow, low-velocity [O I] ^1D–^3P lines at 6300 Å showing signs of Keplerian rotation (*Bally et al.*, 1998; *Acke et al.*, 2005). The excited O ^1D atoms most likely result from photodissociation of
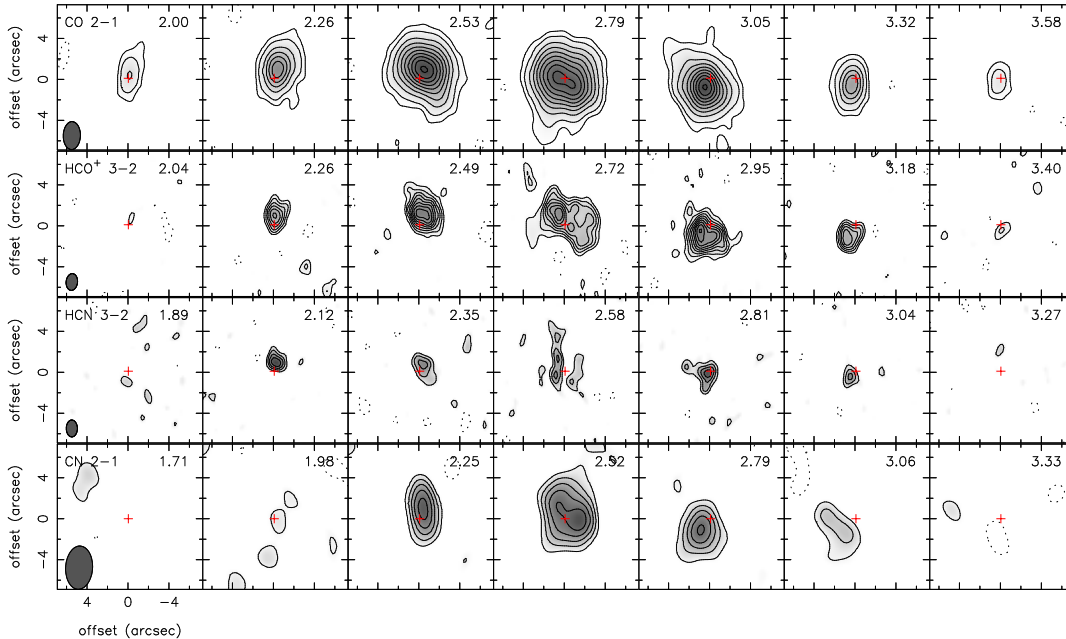
Fig. 4.— SMA channel maps of the millimeter and submillimeter spectral line emission from the TW Hya circumstellar disk. The ellipses at lower left in each series of panels display the synthesized beam, which for the HCN 3-2 observations achieves an effective spatial resolution of ~60 AU. Kindly provided by C. Qi in advance of publication (*Qi et al.* 2006, in prep.).

OH in the upper flaring layers of the disk out to at least 10 AU (*Störzer and Hollenbach*, 1998, *van Dishoeck and Dalgarno*, 1984). The OH abundance required to explain the observed [O I] fluxes is $\sim 10^{-7} - 10^{-6}$, significantly larger than that found in current chemical models.

The main reservoir of the gas in disks is H_2, which has its fundamental rotational quadrapole lines at mid-IR wavelengths. Searches for these lines have been performed by *Thi et al.* (2001) with *ISO*, but tentative detections have not been confirmed by subsequent ground-based data (e.g., *Richter et al.*, 2002, *Sako et al.*, 2005), although H_2 vibrational lines have been detected (*Bary et al.*, 2003). Constraining the amount of gas in disks is important not only for Jovian planet formation, but also because the gas/dust ratio affects the chemistry and thermal balance of the disk as well as the dust dynamics.

3.2. Millimeter- and Submillimeter-wave Spectroscopy

At long wavelengths, where the dust emission is largely optically thin, rotational line emission forms a powerful probe of the physics and chemistry in disks. Indeed, at a fiducial radius of 100 AU, with a temperature of 20-30 K, the disk radiates preferentially at (sub)millimeter wavelengths. Surveys of the mm-continuum and SEDs from disks (*Beckwith et al.*, 1990) have confirmed the spatio-temporal properties of dust disks. However, only a *handful* of objects have been investigated by detailed imaging, with mm-wave interferometer observations of CO from disks around T Tauri stars providing among the earliest and most conclusive evidence for the expected ~Keplerian velocity fields (see *Koerner et al.*, 1993, *Dutrey et al.*, 1994).

From such studies a suite of disks have been identified that are many arc seconds in diameter, either because they are nearby (TW Hya) or are intrinsically large (GM Aur, LkCa 15, DM Tau). The age, large size, and masses of these disks make them important for further study since they may represent an important transitional phase in which viscous disk spreading and dispersal competes with planetary formation processes. Their large size makes them difficult, but feasible, targets for further chemical study. Work in this area began with the pioneering observations of DM Tau and GG Tau with the IRAM 30m telescope (*Dutrey et al.*, 1997) and TW Hya with the JCMT (*Kastner et al.*, 1997). Further detections of the higher$-J$ lines of high dipole moment species such as HCN and HCO^+ along with statistical equilibrium analyses demonstrated that the line emission arises from the warm molecular layer with $n_{H_2} \approx 10^6$–10^8 cm^{-3}, $T \gtrsim 30$ K (*van Zadelhoff et al.*, 2001). The very deepest integrations have begun to reveal more complex species (*Thi et al.* 2004), though the larger organics often seen toward protostellar hot cores remain out of reach of existing single dish telescopes.

At present, aperture synthesis observations can only sense the outer disk ($r > 30 - 50$ AU, *Dutrey and Guilloteau*, 2004; see the chapter by *Dutrey et al.*) for stars in the nearest molecular clouds. Thus, the *chemical* imaging of disks is rarer still, with studies concentrating on a few of the best characterized T Tauri and Herbig Ae stars. Imaging studies of LkCa 15, for example, have detected a number of isotopologues of CO along with the molecular ions HCO^+

and N_2H^+ and the more complex organics formaldehyde and methanol (*Duvert et al.*, 2000, *Aikawa et al.*, 2003, *Qi et al.*, 2003). For this disk at least, molecular depletion of molecules onto the icy mantles of grains near the disk midplane is found to be extensive, but the fractional abundances and ionization in the warm molecular layer are in line with those seen toward dense PDRs (Section 2.1). While the lines from the less abundant species can be detected, they were too weak to image with good signal-to-noise. Thus, while millimeter-wave rotational line emission is a good tracer of the outer disk velocity field it is not a robust tracer of the mass unless the chemistry is very well understood.

New observational facilities are poised to change this situation dramatically, as illustrated by the recent SMA results on the TW Hya disk presented in Figure 4 (*Qi et al.* 2006, in prep.). At a distance of only 56 pc, observations of this source provide nearly 2–3 times the effective linear resolution of studies in Taurus and Ophiuchus. Thus, channel maps such as those presented can be used to derive a great deal about the physical and chemical structure of the disk - its size and inclination (*Qi et al.* 2004), the run of mass surface density and temperature with radius, the chemical abundance ratios with radius in the outer disk, etc. Ongoing improvements to existing arrays such as the eSMA, PdBI, and CARMA will enable similar studies for a large number of disks in the near future, and will push the radii over which chemical studies can be pursued down to 10-20 AU. Resolving the chemical gradients discussed in §4.3 and 4.4 and studying the chemistry in the 1-10 AU zone of active planet formation will require even greater sensitivity and spatial resolution, and awaits ALMA.

4. CHEMICAL AND PHYSICAL LINKS

Protoplanetary disks are evolving in many different, but connected, ways. Small micron sized dust grains collide, coagulate, collisionally fragment, and settle in a process that ultimately produces planets (*Weidenschilling*, 1997). At the same time the disk is viscously evolving, with indications that the disk mass accretion rate decreases with age (*Hartmann et al.*, 1998). Finally, disks evolve chemically, with the eventual result that all heavy elements are frozen on grains in the midplane and, prior to gas dissipation, chemistry consists of H_2 ionization and the deuteration sequence to H_2D^+, D_2H^+, and D_3^+ (see Section 4.3 and Section 5). The interconnections between these types of evolution is, at present, poorly understood. Nonetheless, some physical and chemical connections have become clear, which we review here.

4.1. Grain Evolution

The onset of grain evolution within a protoplanetary disk consists of collisional growth of sub-micron sized particles into larger grains; the process continues until the larger grains decouple from the gas and settle to an increasingly dust-rich midplane (*Nakagawa et al.*, 1981; *Weidenschilling and Cuzzi*, 1993; *Beckwith et al.*, 2000). Evolv-

ing dust grains within irradiated disks reprocess stellar and accretion-generated UV and optical photons into the IR and sub-mm. Thus, the dust thermal emission spectrum bears information on the grain size distribution and spatial location. This, together with the spectral features discussed in Section 3.1.1, is used to provide evidence for grain evolution in ∼1 Myr T Tauri systems (*Beckwith et al.* 2000, see the chapter by *Dullemond et al.*, and references therein).

Grain coagulation can alter the chemistry through the reduction in the total geometrical cross-section, lowering the adsorption rate and the Coulomb force for ion-electron grain recombination. Micron-sized grains couple to the smallest scales of turbulence (*Weidenschilling and Cuzzi*, 1993) and have a thermal, Brownian, velocity distribution. Thus, the timescale of grain-grain collisions is, $\tau_{gr-gr} \propto a_d^{5/2}/(T_d^{1/2}\xi n_H)$, where a_d is the grain radius, ξ the gas-to-dust mass ratio, and T_d the dust temperature (*Aikawa et al.*, 1999). In this fashion grain coagulation proceeds faster at small radii where the temperatures and densities are higher. *Aikawa et al.* (1999) note that the longer timescale for adsorption on larger grains leaves more time for gas-phase reactions to drive toward a steady-state solution; this involves more carbon trapped in CO as opposed to other more complex species.

Overall, the evolution of grains, both coagulation and sedimentation, can be a controlling factor for the chemistry. As grains grow the UV opacity, which is dominated by small grains, decreases, allowing greater penetration of ionizing/dissociating photons (e.g., *Dullemond and Dominik* 2005). As an example, in the coagulation models of *Dullemond and Dominik* (2005) the integrated vertical UV optical depth at 1 AU decreases over several orders of magnitude, towards optically thin over the entire column (see also *Weidenschilling*, 1997). The chemical effects are demonstrated in Fig. 5(b) where we show the C^+ to CO transition as a function of vertical distance for two dust models, well-mixed and settled (*Jonkheid et al.* 2004). In the settled model the CO transition occurs at slightly smaller height, even though this model assumes PAH's remain present in the upper atmosphere. Thus as grains evolve there will be a gradual shifting of the warm molecular layer deeper into the disk, eventually into the midplane. Because the grain emissivity, density, and temperature will also change, the chemical and emission characteristics of this layer may be altered (*Aikawa and Nomura*, 2006). These effects are magnified in the inner disk, where there is evidence for significant grain evolution in a few systems (*Uchida et al.*, 2004; *Calvet et al.*, 2005) and deeper penetration of energetic radiation (*Bergin et al.*, 2004). A key question in this regard is the number of small grains (e.g., PAHs) present in the atmosphere of the disk during times when significant coagulation and settling has occurred (e.g., *Dullemond and Dominik*, 2005; *D'Alessio et al.*, 2006).

It is worth noting that the penetration of X-ray photons is somewhat different than those at longer UV wavelengths. Absorption of UV radiation is dominated by the
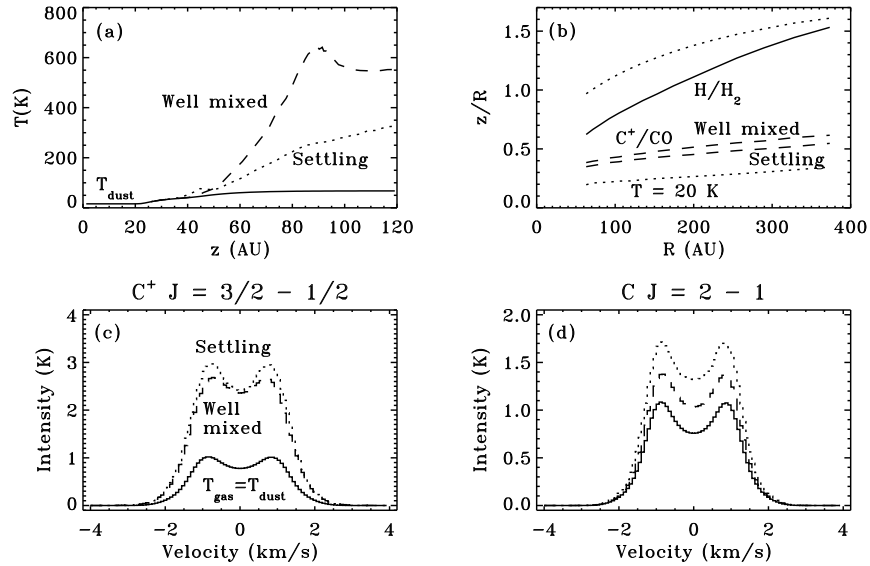
Fig. 5.— (a) Vertical distribution of gas (well mixed model: dashed line; settling model: dotted line) and dust temperatures (solid line). (b) Vertical chemical structure with the edge of the disk and 20 K isotherm as dotted lines, the H/H$_2$ transition as a solid line and the C$^+$/CO transitions in dashed lines (for both well mixed and settled models). (c) C$^+$ 158 μm emission and (d) C 370 μm emission lines for $T_g = T_d$ (solid), and T_g calculated independently for well mixed (dashed) and settling (dotted) models. Taken from *Jonkheid et al.* (2004).

small grains, while X-rays are absorbed at the atomic scale by heavy metals predominantly trapped in the grain cores. Thus, coagulation will have a greater effect on UV photons. When the grain mass is distributed downwards by settling, the X-ray penetration depth increases, eventually to the limit of total heavy element depletion where the opacity at 1 keV decreases by a factor of ~ 4.5 (i.e. the H and He absorption limit; *Morrison and McCammon*, 1983).

4.2. Gas Thermal Structure

Models of disk physical structure have generally assumed that dust and gas temperatures are in equilibrium (*Chiang and Goldreich*, 1997; *D'Alessio et al.*, 1998). However, the disk vertical structure is set by the temperature of the dominant mass component, hydrogen, which under some conditions in the upper disk atmosphere is thermally decoupled from dust (*Chiang and Goldreich*, 1997).

Irradiated disk surfaces are analogs to interstellar PDRs, which have a history of detailed thermal balance calculations (see *Hollenbach and Tielens*, 1999 and references therein). In the studies of the gas thermal balance in disk atmospheres (*Jonkheid et al.* 2004; *Kamp and Dullemond* 2004; *Nomura and Millar* 2005) a number of heating mechanisms have been investigated: including photoelectric heating by PAHs and large grains, UV excitation of H$_2$ followed by collisional de-excitation, H$_2$ dissociation, H$_2$ formation, gas-grain collisions, carbon ionization, and cosmic rays. In decoupled layers, the gas cools primarily by atomic ([O I], [C II], [C I]) and molecular (CO) emission, with the dominant mechanism a function of radial and ver-

tical distance.

A sample of these results are shown in Fig. 5; note that the gas temperature can exceed that of the dust in the upper atmosphere (Fig. 5a), which has consequences for the gas phase emission (Fig. 5c,d). The inclusion of PAHs into the models has an effect as PAHs provide additional heating power and are strong UV absorbers. Thus, grain evolution can significantly alter the thermal structure (see Fig. 5) by removing PAHs and small grains through coagulation and larger grains by settling, reducing photoelectric heating. In disks where grains have grown to micron size, and which are optically thin to UV radiation, other heating processes such as the drift velocity between the dust and gas may become important (see *Kamp and van Zadelhoff*, 2001).

One of the largest chemical influences for most of the disk mass is the freeze-out of molecular species onto grain surfaces. In general, the loss of gas coolants would produce a temperature rise, but in (mid-plane) layers dominated by freeze-out, the densities are high enough to thermally couple the gas to the dust (see, e.g., *Goldsmith*, 2001).

4.3. The Ionization Fraction

Over the past few years the disk fraction ionization has received a high degree of attention owing to the appreciation of the Magneto-Rotational Instability (MRI) as a potential mechanism for disk angular momentum transport (e.g., *Balbus and Hawley*, 1991; *Stone et al.*, 2000). The chemical evolution is linked to dynamics as the presence of ions is necessary to couple the gas to the magnetic field. As we will outline, most of the ionization processes are active at

9

TABLE 1
DISK IONIZATION PROCESSES AND VERTICAL ION STRUCTURE

Layer/Carrier	Ionization Mechanism	$\Sigma_{\tau=1}$ (g cm^{-2})[a]	α_r (cm^{-3}s^{-1})[b]	x_e^c
Upper Surface H$^+$	UV photoionization of H[d] $k_{H^+} \sim 10^{-8}$ s^{-1}	6.9×10^{-4}	$\alpha_{H^+} = 2.5 \times 10^{-10} T^{-0.75}$	$> 10^{-4}$
Lower Surface C$^+$	UV photoionization of C[e] $k_{C^+} \sim 4 \times 10^{-8}$ s^{-1}	1.3×10^{-3}	$\alpha_{C^+} = 1.3 \times 10^{-10} T^{-0.61}$	$\sim 10^{-4}$
Warm Mol. H$_3^+$,HCO$^+$	Cosmic-[f] and X-Ray[g] Ionization $\zeta_{cr} = \frac{\zeta_{cr,0}}{2}[\exp(-\frac{\Sigma_1}{\Sigma_{cr}}) + \exp(-\frac{\Sigma_2}{\Sigma_{cr}})]$ $\zeta_X = \zeta_{X,0} \frac{\sigma(kT_X)}{\sigma(1keV)} L_{29} J(r/AU)^{-2}$	96 (CR) 0.008 (1keV) 1.6 (10 keV)	$\alpha_{H_3^+} = -1.3 \times 10^{-8}+$ $1.27 \times 10^{-6} T^{-0.48}$ $\alpha_{HCO^+} = 3.3 \times 10^{-5} T^{-1}$	$10^{-11 \rightarrow -6}$
Mid-Plane	Cosmic-ray[f] and Radionuclide[h] $\zeta_R = 6.1 \times 10^{-18}$ s^{-1}			
Metal$^+$/gr	($r < 3$ AU)		$\alpha_{Na^+} = 1.4 \times 10^{-10} T^{-0.69}$	$< 10^{-12}$
HCO$^+$/gr	($3 < r < 60$ AU)		α_{gr} (see text)	$10^{-13,-12}$
H$_3^+ -$D$_3^+$	($r > 60$ AU)		$\alpha_{D_3^+} = 2.7 \times 10^{-8} T^{-0.5}$	$> 10^{-11}$

[a] Effective penetration depth of radiation (e.g., $\tau = 1$ surface).

[b] Recombination rates from UMIST database (*Le Teuff et al.*, 2000), except for H$_3^+$ which is from *McCall et al.* (2004) and D$_3^+$ from *Larsson et al.* (1997).

[c] Ion fractions estimated from *Semenov et al.* (2004) and *Sano et al.* (2000). Unless noted values are relevant for all radii.

[d] Estimated at 100 AU assuming 10^{41} s^{-1} ionizing photons (*Hollenbach et al.*, 2000) and $\sigma = 6.3 \times 10^{-18}$ cm^2 (H photoionization cross-section at threshold). This is an overestimate as we assume all ionizing photons are at the Lyman limit.

[e] Rate at the disk surface at 100 AU using the radiation field from *Bergin et al.* (2003).

[f] Taken from *Semenov et al.* (2004). $\zeta_{cr,0} = 1.0 \times 10^{-17}$ s^{-1} and $\Sigma_1(r,z)$ is the surface density above the point with height z and radius r with $\Sigma_2(r,z)$ the surface density below the same point. $\Sigma_{cr} = 96$ g cm^{-2} as given above (*Umebayashi and Nakano*, 1981).

[g] X-ray ionization formalism from *Glassgold et al.* (2000). $\zeta_{X,0} = 1.4 \times 10^{-10}$ s^{-1}, while $L_{29} = L_X/10^{29}$ erg s^{-1} is the X-ray luminosity and J is an attenuation factor, $J = A\tau^{-a} e^{-B\tau^b}$, where $A = 0.800$, $a = 0.570$, $B = 1.821$, and $b = 0.287$ (for energies around 1 keV and solar abundances).

[h] ^{26}Al decay from *Umebayashi and Nakano* (1981). If ^{26}Al is not present ^{40}K dominates with $\zeta_R = 6.9 \times 10^{-23}$ s^{-1}.

the surface and there exists the potential that accretion may only be active on the surface (*Gammie*, 1996, but see also *Klahr and Bodenhiemer*, 2003; *Inutsuka and Sano*, 2005).

In equilibrium, the ion fraction, $x_e = n_e/n_H$, can be expressed by: $x_e = \sqrt{\zeta/(\alpha_r n_H)}$, where ζ is the ionization rate and α_r the electron recombination rate. In Table 1 we provide an overview of disk ionization. The top left panel in Fig. 6 also shows the electron abundance (equivalent to the ionization fraction) from a detailed model (*Semenov et al.*, 2006, in prep.). This figure, along with Table 1, can be used as a guide for the following discussion. For a discussion of the validity of the equilibrium assumption see *Semenov et al.* (2004), while *Ilgner and Nelson* (2005a) provide a detailed comparison of ionization and MRI for a variety of reaction networks.

The observed FUV radiation excess produces high ion fractions, but only over a small surface column, with C$^+$ as the charge carrier (the ionized hydrogen layer will be quite small). Deeper inside the warm molecular layer is reached, where primary charge carriers are molecular ions produced by X-ray ionization of H$_2$ (*Glassgold et al.*, 1997) and, when this decays, cosmic ray ionization. It is worth noting that X-ray flares are observed in T Tauri systems (e.g., *Favata et al.*, 2005), after which there will exist a burst of ionization on the disk surface that will last for $\tau_r \sim 1/(\alpha_r n_e)$.

An important question is whether cosmic rays penetrate the inner disk. Within our own planetary system, the Solar wind excludes ionizing cosmic rays. Estimates of mass loss rates from young star winds significantly exceed the Solar mass loss rate (*Dupree et al.*, 2005), and may similarly exclude high energy nuclei. In the case of cosmic ray penetration, primary charge carriers range from metal ions and/or grains at small radii (~ 1 AU) to molecular ions for $r > $ few AU with $x_e \sim 10^{-13}$ near the midplane. If ionizing cosmic rays are excluded, radionuclides can produce $x_e \sim 10^{-3}(T/20 \text{ K})^{-0.5}/\sqrt{n_H}$ (assuming H$_3^+$ as the dominant ion and ^{26}Al is present; if ^{26}Al is not present the pre-factor is 10^{-8}). The presence or absence of metal ions in the midplane can also affect MHD driven dynamics (*Ilgner and Nelson*, 2005b). Metal ions have recombination times longer than molecular ions or the diffusive timescale and, if present, can be important charge reservoirs.

In dense protostellar cores models and observations now suggest near total freeze-out of heavy species that results in D$_3^+$ and other forms of deuterated H$_3^+$ becoming important charge carriers (*Roberts et al.*, 2004; *Walmsley et al.*, 2004). The disk midplane should present a similar environment. The recent detection of H$_2$D$^+$ by *Ceccarelli et al.* (2004) in the outer disks of TW Hya and DM Tau, supports this view.

In the midplane one issue is the electron sticking coefficient (S_e) to grains. *Sano et al.* (2000) assume $S_e = 0.6$ based on the work of *Nishi et al.* (1991), while *Semenov et al.* (2004) assume a strong temperature dependence with S_e essentially zero at high temperatures. Thus in the inner disk
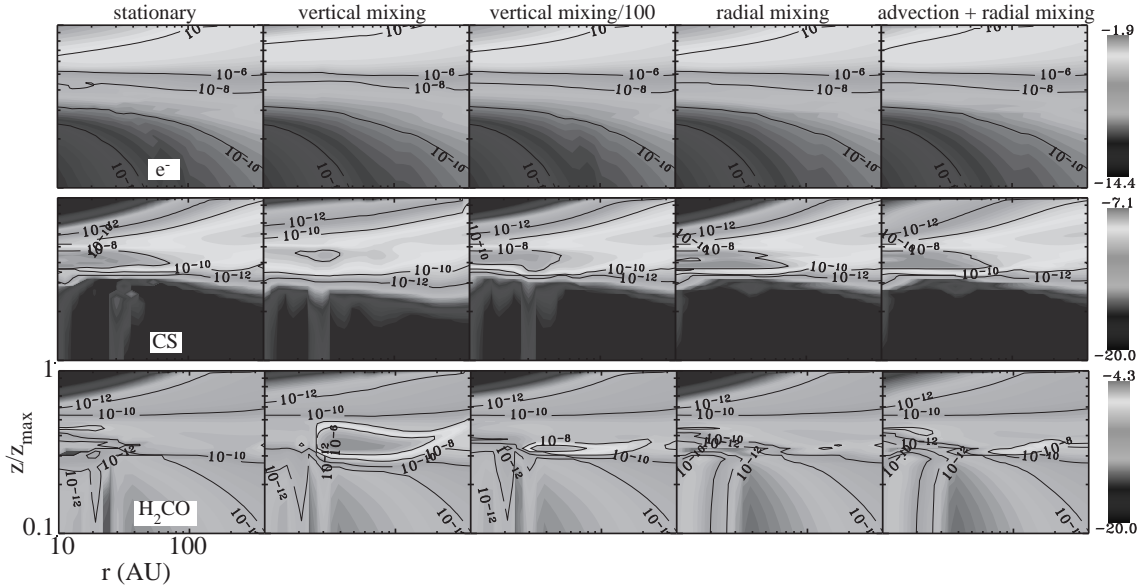
Fig. 6.— Shown are molecular abundances in the 2D flared disk of *D'Alessio et al.* (1999) after 10^6 years of the evolution. The x-axis represents radii from 10 to 370 AU on logarithmic scale, while y-axis corresponds to normalized vertical extend of the disk, z/z_{max}, that ranges from 0.1 to 1.0 on logarithmic scale. The abundance values are given in respect to the total amount of hydrogen nuclei. Several models with variable mixing were considered and are labeled above each panel (note: vertical mixing/100 is a model with reduced mixing). Kindly provided by D. Semenov in advance of publication (*Semenov et al.*, 2006, in prep.).

the primary charge carrier differs between these two models with grains dominating in the *Sano et al.* (2000) model and molecular/metal ions in the *Semenov et al.* (2004) model (for a discussion of electron sticking coefficients see *Weingartner and Draine*, 2001). If grains are the dominant charge carrier the recombination rate α_{gr} is the grain collisional timescale with a correction for long-distance Coulomb focusing: $\alpha_{gr} = \pi a_d^2 n_{gr} v (1 + e^2/k a_d T_d)$. At $T_d = 20$ K *Draine and Sutin* (1987) show that for molecular ions, grain recombination will dominate when $n_e/n_H < 10^{-7}(a_{min}/3\text{Å})^{-3/2}$. Grains can be positive or negative and carry multiple charge: *Sano et al.* (2000) find that the total grain charge is typically negative, while the amount of charge is 1-2e^-, varying with radial and vertical distance. Since the criteria for the MRI instability include the mass of the charged particles, it is important to determine whether grains or molecules are the primary charge carriers.

4.4. Mixing

Chemical mixing within the solar nebula has a long history due to important questions regarding the potential transport of material from warm, thermochemically active, regions (either inner solar nebula or Jovian sub-nebula) into colder inactive regions (*Lewis and Prinn*, 1980, *Prinn and Fegley*, 1981). It is clear that some movement of processed material is likely, for example the detection of crystalline silicates in comets (*Crovisier et al.*, 1997; *Bockelée-Morvan et al.*, 2000) and the chondritic refractory inclusions in meteorites (*MacPherson et al.*, 1988) implies some mixing. However, the mixing efficiency has been a matter of debate

(*Stevenson*, 1990; *Prinn*, 1990; 1993).

In terms of the dynamical movement of gas within a protoplanetary disk and its chemical effects, a key question is whether the chemical timescale, τ_{chem}, is less than the relevant dynamical timescale, τ_{dyn}, in which case the chemistry will be in equilibrium and unaffected by the motion. If $\tau_{dyn} < \tau_{chem}$ then mixing will alter the anticipated composition. These two constraints are the equilibrium and disequilibrium regions (respectively) outlined in *Prinn* (1993). What is somewhat different in our current perspective is the recognition of an active gas-phase chemistry on a photon-dominated surface. This provides another potential mixing reservoir in the vertical direction, as opposed to radial, which was the previous focus.

It is common to parameterize the transfer of angular momentum in terms of the turbulent viscosity, $\nu = \alpha c_s H$, where ν is the viscosity, c_s the sound speed, H the disk scale height, and α is a dimensionless parameter (*Shakura and Sunyaev*, 1973; *Pringle*, 1981). *Hartmann et al.* (1998) empirically constrained the α-parameter to be $\lesssim 10^{-2}$ for a sample of T Tauri disks.

The radial disk viscous timescale is $\tau_\nu = r^2/\nu$ or,

$$\tau_\nu \sim 10^4 \text{yr} \left(\frac{\alpha}{10^{-2}}\right)^{-1} \left(\frac{T}{100\,\text{K}}\right)^{-1} \left(\frac{r}{1\,\text{AU}}\right)^{\frac{1}{2}} \left(\frac{M_*}{M_\odot}\right)^{\frac{1}{2}}.$$

The diffusivity, D, is not necessarily the same as the viscosity, ν (e.g., *Stevenson*, 1990), even though some treatments equate the two (*Ilgner et al.*, 2004; *Willacy et al.*, 2006). In the case of MRI, *Carballido et al.* (2005) estimate $\nu/D \sim 11$, i.e., turbulent mixing is much less efficient

11

than angular momentum transport (but, see also *Turner et al.* 2006 where $\nu/D \sim 1 - 2$). With knowledge of the ν/D ratio, the above equation for τ_ν serves as an estimate of the dynamical timescale for diffusion.

Recent models that include dynamics with chemistry generally can be grouped into two categories. Ones that include only advection (*Duschl et al.*, 1996; *Finocchi et al.*, 1997; *Willacy et al.*, 1998; *Aikawa et al.*, 1999; *Markwick et al.*, 2002) and ones that investigate the effects of vertical and/or radial mixing including advection (*Wehrstedt and Gail*, 2003; *Ilgner et al.*, 2004; *Willacy et al.*, 2006; *Semenov et al.*, 2006, in prep.). The effects of advection on the chemical evolution are dominated by migration of icy grains towards the warmer inner disk where the volatile ices evaporate. Most of the species that desorb are processed via the active gas phase and/or gas-grain chemistry into less volatile species that freeze out (e.g., *Aikawa et al.*, 1999). For instance, N_2 evaporates at $T > 20$ K (Öberg et al. 2005) and is converted to HCN, and other less volatile species, via ion-molecule reactions. This would predict a strong temporal dependence on the chemistry in the accreting material within the evaporative zones.

As an example of more complex dynamical models, Fig. 6 shows results from *Semenov et al.* (2006, in preparation), but see also *Willacy et al.* (2006). For these models, radial and vertical mixing is incorporated into a disk model that also includes all other relevant physical/chemical processes described in Section 1.2. The model assumes a traditional alpha-disk that is fully dynamically active with $\nu/D = 1$. This model reproduces the basic structure shown in Fig. 1, with the presence of a warm molecular layer and a drop in abundance towards the mid-plane (most dramatically seen in CS). When vertical transport and/or radial transport is included the essential features of the basic structure are preserved, in the sense that the warm molecular layer still exists, although it may be expanded (*Willacy et al.* 2006). This is readily understood as the chemical timescales driven by the photodissociation, $\tau_{\text{chem}} \lesssim 100 - 1000(r/100 \text{ AU})^2$ yrs, are less than the dynamical timescale at all radii, thus the photo-chemical equilibrium is preserved. The effects of radial mixing and advection are mostly important for the upper disk atmosphere. Two results stand out. (1) The electron abundance structure shows little overall change. Thus ionization equilibrium is preserved throughout the disk. (2) There is clear evidence for abundance enhancements of key species (such as H_2CO) in models with vertical mixing. The molecules with the largest abundance enhancements in the vertical mixing models are those that are more volatile than water, but are also major components of the grain mantle. This suggests that observations of these species may ultimately be capable of constraining disk mixing.

However, all predictions are highly uncertain. If MRI powers accretion, and cosmic rays do not penetrate to the midplane, then the bulk of the disk mass will not participate in any global mixing. Moreover, the outer disk may be actively turbulent while the inner disk may be predominantly quiescent (excluding the surface ionized by X-rays). Thus, while current models are suggestive of the importance of mixing for the disk chemical evolution, significant questions remain.

5. Deuterated Species in Disks and Comets

Isotopic fractionations are measured in primordial materials in comets and meteorites, and considered to be good tracers of their origin and evolution. Here we review recent progress on deuterium fractionation in relation to comets (see the chapter by Yurimoto et al. for a discussion of oxygen fractionation). In Table 2 we list molecular D/H ratios, defined as $n(XD)/n(XH)$, observed in protoplanetary disks, comets and low-mass cores.

The two-dimensional $(r - z)$ distributions of deuterated species at $r \geq 26$ AU have been calculated in models of *Aikawa and Herbst* (2001) and *Aikawa et al.* (2002). At low temperatures D/H fractionation proceeds via ion-molecule reactions; species such as H_3^+ and CH_3^+ are enriched in deuterium because of the difference in zero-point energies between isotopomers and rapid exchange reactions such as $H_3^+ + HD \rightarrow H_2D^+ + H_2$ (e.g., *Millar et al.*, 1989). Since CO is the dominant reactant with H_2D^+, CO depletion further enhances the H_2D^+/H_3^+ ratio. The deuterium enrichment propagates to other species via chemical reactions (see the chapters by *Ceccarelli et al.* and *Di Francesco et al.*). Hence the D/H ratios of HCN and HCO^+ tend to increase towards the midplane with low temperature and heavy molecular depletion, while their absolute abundances reach the maximum value at some intermediate height. The column density D/H ratios of HCO^+, HCN and H_2O integrated in the vertical direction are 10^{-2} at $r \gtrsim 100$ AU and 10^{-3} at 26 AU $\lesssim r \lesssim 100$ AU in *Aikawa et al.* (2002). H_3^+ and its deuterated families (H_2D^+, HD_2H^+ and D_3^+), on the other hand, are abundant in the midplane, and the D/H ratio can even be higher than unity. At present, the data on D/H ratios in disks (with both deuterated and hydrogenated species observed) is limited to the detection of DCO^+ (*van Dishoeck et al.*, 2003), which is in agreement with models (*Aikawa et al.*, 2002).

In contrast to the mm observations of gas in the outer disk, comets carry information on ice (rather than gas) at radii of $5 - 30$ AU (e.g., *Mumma et al.*, 1993). The similarity in molecular D/H ratios between comets and high-mass hot cores has been used to argue for an interstellar origin of cometary matter, but the D/H ratios in low-mass star-forming regions (e.g., TMC-1) are higher than those in comets, casting questions as to the interstellar origin scenario (e.g., *Irvine et al.*, 1999). In recent years hot cores are found around low- or intermediate-mass protostars (see IRAS 16293-2422). In addition, temporal and spatial variation in molecular D/H ratios are found in low-mass dense cores, where the bulk of ices formed (e.g., *Bacmann et al.*, 2003; *Caselli*, 2002). Hence, what one means by "interstellar" is ambiguous. Eventually, molecular evolution from cores to disks and within disks should be investigated.

TABLE 2

D/H RATIOS IN COMETS, DISKS AND CORES

Region Type	Object	Species	D/H ratio	Reference
Hot cores	various	HDO	3.0×10^{-4}	*Gensheimer et al.* (1996)
	various	DCN	$0.9 - 4.0 \times 10^{-3}$	*Hatchell et al.* (1998)
Low-mass protostars	IRAS 16293-2422	HDO	3.0×10^{-2}	*Parise et al.* (2005)
	IRAS 16293-2422	CH_3OD	2.0×10^{-2}	*Parise et al.* (2002)
	IRAS 16293-2422	CH_2DOH	3.0×10^{-1}	*Parise et al.* (2002)
	various	HDCO	$5.0 - 7.0 \times 10^{-2}$	*Roberts et al.* (2002)
	various	NH_2D	$1.0 - 2.8 \times 10^{-1}$	*Roueff et al.* (2005)
	various	DCO^+	1.0×10^{-2}	Class 0 average; *Jørgensen et al.* (2004)
	various	DCN	1.0×10^{-2}	Class 0 average; *Jørgensen et al.* (2004)
Dark Cores	L1544	DCO^+	4.0×10^{-2}	*Caselli et al.* (2002)
	L134N	DCO^+	1.8×10^{-1}	*Tiné et al.* (2000)
	TMC-1	DCN	2.3×10^{-2}	*van Dishoeck et al.* (1993)
Disks	TW Hya	DCO^+	3.5×10^{-2}	*van Dishoeck et al.* (2003)
	LkCa 15	HDO	6.4×10^{-2}	*Kessler et al.* (2003)
	DM Tau	HDO	1.0×10^{-3}	*Ceccarelli et al.* (2005), *Dominik et al.* (2005)
	LkCa 15	DCN	< 0.002	*Kessler et al.* (2003)
Comets	Halley	HDO	$(3.2 \pm 0.3) \times 10^{-4}$	*Eberhardt et al.* (1995)
	Hyakutake	HDO	$(2.9 \pm 1.0) \times 10^{-4}$	*Bockelée-Morvan et al.* (1998)
	Hale-Bopp	HDO	$(3.3 \pm 0.8) \times 10^{-4}$	*Meier et al.* (1998)
	Hale-Bopp	HDO	2×10^{-3}	*Blake et al.* (1999)
	Hale-Bopp	DCN	$(2.3 \pm 0.4) \times 10^{-3}$	*Meier et al.* (1998)

NOTE.—HDO has only been *tentatively* detected in disks, whereas H_2O has not. In these cases (*Ceccarelli et al.*, 2005; *Kessler et al.*, 2003) the D/H ratio is estimated by model calculation and is therefore highly uncertain.

Aikawa and Herbst (1999) calculated molecular abundances and D/H ratios in a fluid parcel accreting from a core to the disk, and then from the outer disk radius to the comet-forming region (30 AU), showing that ratios such as DCN/HCN depend on the ionization rate in the disk, and can decrease from 0.01 to 0.002 (if the migration takes 10^6 yr and the ionization rate is 10^{-18} s^{-1}) due to chemical reactions during migration within the disk. This model, however, assumed that the fluid parcel migrates only inward within the cold ($T \lesssim 25$ K) midplane, which results in the survival of highly deuterated water accreted from the core. *Hersant et al.* (2001) solved the diffusion equation to obtain the D/H ratio in the disk; initially high D/H ratios of H_2O and HCN are lowered by mixing with the poorly deuterated material from the smaller radii. This model, however, considered only thermal reactions. In reality deuterium fractionation (or backward reactions) via ion-molecule reactions would proceed within the disk depending on the local ionization rate, temperature, and degree of molecular depletion, while the vertical and radial diffusion will tend to lessen the spatial gradient of D/H ratios. Inclusion of deuterated species in the recent models with non-thermal chemistry and 2-D diffusion is desirable.

6. Outstanding Issues and Future Prospects

Significant gains have been made in our observational and theoretical understanding of the chemical evolution of protoplanetary disks in the decade since the last review in this conference series. We now recognize the importance of the irradiated surface, which at the very least contains an active chemistry and is responsible for most observed molecular emission lines. The gross characteristics and key ingredients of this surface are roughly understood. How the varied effects (grain evolution, UV/X-ray radiation dominance, etc..) play out on the chemical evolution in terms of X-ray/UV dominance and the dependence on other evolutionary factors, is one of the challenges for future models. Given the observed chemical complexity, a detailed understanding of the chemistry is a pre-requisite for the interpretation of ongoing and future observations of molecular emission in protoplanetary disks.

Disk surface processes may dominate the observed chemistry, but it is not certain how much of a role this chemistry plays in altering the chemical characteristics within the primary mass reservoir, the disk midplane. Thus one of the main outstanding questions for disk chemistry remains: how much material remains pristine and chemically unaltered from its origin in the parent molecular cloud. We now have observational and theoretical evidence for active chemical zones; thus it is likely that the most volatile species, which are frozen on grains in the infalling material (e.g., CO, N_2) do undergo significant processing. This will trickle down to other, less abundant molecules that form easily from the "parent species" (e.g., H_2CO, HCN and the deuterated counterparts). Disentangling these effects

will be complicated because the chemistry in the outer disk ($r > 30$ AU), which through advection feeds the inner disk, is quite similar to that seen in dense regions of the interstellar medium. For the least volatile molecules, in particular water ice, sublimation and subsequent gas-phase alteration is less likely, unless there is significant radial mixing from the warmer inner disk to colder outer regions.

In part, our recognition of the warm molecular layer and the importance of photo-chemistry, is driven by our current observational facilities, which are unable to resolve the innermost regions of the disk (e.g., planet forming zones), coupling better to the larger surface area of the outer disk. Within $r < 10$–30 AU, the midplane and surface are both hot enough to sublime even the least volatile molecules (e.g., H_2O), eventually producing an active chemistry that is described by the earlier PP III review (*Prinn*, 1993) and in the chapter by Najita et al. The transition between these layers, the so-called "snow-line" and the chemistry within the planet forming zone, will be species specific and should be readily detectable with upcoming advances in our capabilities, in particular the eagerly awaited ALMA array.

In summary, we stand on the cusp of the marriage of a rapidly emerging new field, studies of extra-solar protoplanetary disk chemical evolution, and an old one, the cosmochemical study of planets, meteorites, asteroids, and comets. In this review we have outlined broad areas where the evolving chemistry can be altered through changes induced by vertical and horizontal temperature gradients, the evolution of grain properties, and disk dynamics (mixing). Thus studies of active chemistry in extra-solar disks offers the promise and possibility to untangle long-standing questions regarding the initial conditions, chemistry, and dynamics of planet formation, the origin of cometary ices, and, ultimately, a greater understanding of the organic content of gas/solid reservoirs that produced life at least once in the Galaxy.

REFERENCES

Acke, B., van den Ancker, M. E., and Dullemond, C. P. 2005. *Astron. Astrophys., 436*, 209-230.

Acke, B. and van den Ancker, M. E. 2004. *Astron. Astrophys., 426*, 151-170.

Aikawa, Y. and Nomura, H. 2006, Astrophys. J., in press

Aikawa, Y., van Zadelhoff, G. J., van Dishoeck, E. F., and Herbst, E. 2002. *Astron. Astrophys., 386*, 622-632.

Aikawa, Y. and Herbst, E. 2001. *Astron. Astrophys., 371*, 1107-1117.

Aikawa, Y. and Herbst, E. 1999. *Astron. Astrophys., 351*, 233-246.

Aikawa, Y., Umebayashi, T., Nakano, T., and Miyama, S. M. 1999. *Astrophys. J., 519*, 705-725.

Aikawa, Y., Umebayashi, T., Nakano, T., and Miyama, S. M. 1997. *Astrophys. J., 486*, L51.

Alexander, R. D., Clarke, C. J., and Pringle, J. E. 2005. *Mon. Not. Roy. Astron. Soc., 358*, 283-290.

Bacmann, A., Lefloch, B., Ceccarelli, C., Steinacker et. al. 2003. CO *Astrophys. J., 585*, L55-L58.

Balbus, S. A. and Papaloizou, J. C. B. 1999. *Astrophys. J., 521*, 650-658.

Bally, J., Sutherland, R. S., Devine, D., and Johnstone, D. 1998. *Astron. J., 116*, 293-321.

Bary, J. S., Weintraub, D. A., and Kastner, J. H. 2003. *Astrophys. J., 586*, 1136-1147.

Beckwith, S. V. W., Henning, T., and Nakagawa, Y. (2000) In *Protostars and Planets IV* (V. Mannings et al., eds.), pp 533-558. Univ. of Arizona, Tucson.

Beckwith, S. V. W., Sargent, A. I., Chini, R. S., and Guesten, R. 1990. *Astron. J., 99*, 924-945.

Bergin, E., and 11 colleagues 2004. *Astrophys. J., 614*, L133-L136.

Bergin, E., Calvet, N., D'Alessio, P., and Herczeg, G. J. 2003. *Astrophys. J., 591*, L159-L162.

Blake, G. A. and Boogert, A. C. A. 2004. *Astrophys. J., 606*, L73-L76.

Blake, G. A., Qi, C., Hogerheijde, M. R., Gurwell, M. A., and Muhleman, D. O. 1999. *Nature, 398*, 213.

Bockelée-Morvan, D., Gautier, D., Hersant, F., Huré, J.-M., and Robert, F. 2002. *Astron. Astrophys., 384*, 1107-1118.

Bockelée-Morvan, D., and 11 colleagues 1998. *Icarus, 133*, 147-162.

Boogert, A. C. A., Hogerheijde, M. R., and Blake, G. A. 2002. *Astrophys. J., 568*, 761-770.

Bringa, E. M. and Johnson, R. E. 2004. *Astrophys. J., 603*, 159-164.

Brittain, S. D. and Rettig, T. W. 2002. *Nature, 418*, 57-59.

Calvet, N., D'Alessio, P., Hartmann, L., Wilner, D., et al. 2002. *Astrophys. J., 568*, 1008-1016.

Calvet, N. and Gullbring, E. 1998. *Astrophys. J., 509*, 802-818.

Calvet, N., Magris, G. C., Patino, A., and D'Alessio, P. 1992. *Rev. Mex. Astron. Astrofis., 24*, 27.

Carballido, A., Stone, J. M., and Pringle, J. E. 2005. *Mon. Not. Roy. Astr. Soc., 358*, 1055-1060.

Carr, J. S., Tokunaga, A. T., and Najita, J. 2004. *Astrophys. J., 603*, 213-220.

Caselli, P. 2002. *Planetary and Space Science, 50*, 1133-1144.

Caselli, P., Walmsley, C. M., Zucconi, A., Tafalla, M. et al. 2002. *Astrophys. J., 565*, 344-358.

Ceccarelli, C., Dominik, C., Caux, E., Lefloch, B., and Caselli, P. 2005. *Astrophys. J., 631*, L81-L84.

Ceccarelli, C. and Dominik, C. 2005. *Astron. Astrophys., 440*, 583-593.

Ceccarelli, C., Dominik, C., Lefloch, B., Caselli, P., and Caux, E. 2004. *Astrophys. J., 607*, L51-L54.

Chiang, E. I., Joung, M. K., Creech-Eakman, M. J., Qi, C., et al. 2001. *Astrophys. J., 547*, 1077-1089.

Chiang, E. I. and Goldreich, P. 1997. *Astrophys. J., 490*, 368.

Crovisier, J., Bockelée-Morvan, D., Colom, P., Biver, N. et al. 2004. *Astron. Astrophys., 418*, 1141-1157.

Crovisier, J., Leech, K., Bockelée-Morvan, D., Brooke, T. et. al. 1997. *Science, 275*, 1904-1907.

D'Alessio, P., Calvet, N., Hartmann, L., Lizano, S., and Cantó, J. 1999. *Astrophys. J., 527*, 893-909.

D'Alessio, P., Canto, J., Calvet, N., and Lizano, S. 1998. *Astrophys. J., 500*, 411.

Dartois, E., A. Dutrey, and S. Guilloteau 2003. *Astron. Astrophys., 399*, 773-787.

Draine, B. T. and Sutin, B. 1987. *Astrophys. J., 320*, 803-817.

Draine, B. T. 1978, *Astrophys. J. Suppl., 36*, 595-619

Dullemond, C. P. and Dominik, C. 2005. *Astron. Astrophys., 434*, 971-986.

Dullemond, C. P. and Dominik, C. 2004. *Astron. Astrophys., 421*, 1075-1086.

Dupree, A. K., Brickhouse, N. S., Smith, G. H., and Strader, J. 2005. *Astrophys. J., 625*, L131-L134.

Duschl, W. J., Gail, H.-P., and Tscharnuter, W. M. 1996. *Astron. Astrophys., 312*, 624-642.

Dutrey, A. and Guilloteau, S. 2004. *Astrophys. Space Sci., 292*, 407-418.

Dutrey, A., Guilloteau, S., and Simon, M. 1994. *Astron. Astrophys., 291*, L23-L26.

Dutrey, A., Guilloteau, S., and Guelin, M. 1997. *Astron. Astrophys., 317*, L55-L58.

Duvert, G. et al. 2000. *Astron. Astrophys., 355*, 165-170.

Eberhardt, P., Reber, M., Krankowsky, D., and Hodges, R. R. 1995. *Astron. Astrophys., 302*, 301.

Favata, F., Flaccomio, E., Reale, F., Micela, G., Sciortino, S. et. al. 2005. *Astrophys. J., Suppl., 160*, 469-502.

Fegley, B. J. 1999. *Space Sci. Rev., 90*, 239-252.

Fegley, B. J. and Prinn, R. G. (1989) In *The Formation and Evolution of Planetary Systems* (H. Weaver and L. Danly, eds), pp. 171-205. Cambridge Univ., New York

Feigelson, E. D. and Montmerle, T. 1999. *Ann. Rev. Astron. Astrophys., 37*, 363-408.

Finocchi, F. and Gail, H.-P. 1997. *Astron. Astrophys., 327*, 825-844.

Forrest, W. J., and 20 colleagues 2004. *Astrophys. J. Suppl., 154*, 443-447.

Gammie, C. F. 2001. *Astrophys. J., 553*, 174-183.

Gammie, C. F. 1996. *Astrophys. J., 457*, 355.

Gensheimer, P. D., Mauersberger, R., and Wilson, T. L. 1996. *Astron. Astrophys., 314*, 281-294.

Glassgold, A. E., Feigelson, E.D., and Montmerle, T. 2000, In *Protostars and Planets IV* (V. Mannings et al., eds.), pp. 429-456, Univ. of Arizona, Tucson.

Glassgold, A. E., Najita, J., and Igea, J. 2004. *Astrophys. J., 615*, 972-990.

Glassgold, A. E., Najita, J., and Igea, J. 1997. *Astrophys. J., 480*, 344.

Goldsmith, P. F. 2001. *Astrophys. J., 557*, 736-746.

Goto, M., Geballe, T. R., McCall, B. J., Usuda, T. et. al. 2005. *Astrophys. J., 629*, 865-872.

Habart, E., Natta, A., and Krügel, E. 2004. *Astron. Astrophys., 427*, 179-192.

Habing, H. J. 1968. *Bull. Astron. Inst. Neth., 19*, 421.

Hartmann, L., Calvet, N., Gullbring, E., and D'Alessio, P. 1998. *Astrophys. J., 495*, 385.

Hasegawa, T. I. and Herbst, E. 1993. *Mon. Not. Roy. Astro. Soc., 261*, 83-102.

Hatchell, J., Thompson, M. A., Millar, T. J., and MacDonald, G. H. 1998. *Astron. Astrophys. Suppl., 133*, 29-49.

Hawley, J. F. and Balbus, S. A. 1991. *Astrophys. J., 376*, 223.

Hayashi, C. 1981. *Prog. Theor. Phys. Suppl., 70*, 35-53.

Herbig, G. H. and Goodrich, R. W. 1986. *Astrophys. J., 309*, 294-305.

Herbst, E. and Klemperer, W. 1973. *Astrophys. J., 185*, 505-534.

Herczeg, G. J., Wood, B. E., Linsky, J. L., Valenti, J. A., and Johns-Krull, C. M. 2004. *Astrophys. J., 607*, 369-383.

Hersant, F., Gautier, D., and Huré, J.-M. 2001. *Astrophys. J., 554*, 391-407.

Hester, J.J. and Desch, S.J. (2006) In *Chondrites and the Protoplanetary Disk* (A. N. Krot et al., eds.), pp. 107-131. ASP Conf. Series, San Francisco.

Hollenbach, D. J., Yorke, H. W., and Johnstone, D. (2000) In *Protostars and Planets IV* (V. Mannings et al., eds.), pp. 401-429. Univ. of Arizona, Tucson.

Hollenbach, D. J. and Tielens, A. G. G. M. 1999. *Rev. Mod. Phys., 71*, 173-230.

Igea, J. and Glassgold, A. E. 1999. *Astrophys. J., 518*, 848-858.

Ilgner, M. and R. P. Nelson 2005b. *Astron. Astrophys.*, in press.

Ilgner, M. and R. P. Nelson 2005a. *Astron. Astrophys.*, in press.

Ilgner, M., Henning, T., Markwick, A. J., and Millar, T. J. 2004. *Astron. Astrophys., 415*, 643-659.

Inutsuka, S.-i. and T. Sano 2005. *Astrophys. J., 628*, L155-L158.

Irvine, W. M. 1999. *Space Sci. Rev., 90*, 203-218.

Jonkheid, B., Faas, F. G. A., van Zadelhoff, G.-J., and van Dishoeck, E. F. 2004. *Astron. Astrophys., 428*, 511-521.

Jonkheid, B., Kamp, I., Augereau, J.-C., and van Dishoeck, E. F. 2006. *Astron. Astrophys.,* submitted.

Jørgensen, J. K., Schöier, F. L., and van Dishoeck, E. F. 2004, *Astron. Astrophys.*, 416, 603

Kamp, I. and Dullemond, C. P. 2004. *Astrophys. J., 615*, 991-999.

Kamp, I. and van Zadelhoff, G.-J. 2001. *Astron. Astrophys., 373*, 641-656.

Kastner, J. H., Franz, G., Grosso, N., Bally, J. et. al. 2005. *Astrophys. J. Suppl., 160*, 511-529.

Kastner, J. H., Zuckerman, B., Weintraub, D. A., and Forveille, T. 1997. *Science, 277*, 67-71.

Kenyon, S. J. and Hartmann, L. 1987. *Astrophys. J., 323*, 714-733.

Kessler-Silacci, J. E., et al. 2006. *Astrophys. J., 639*, 275-291.

Kessler-Silacci, J. E., Hillenbrand, L. A., Blake, G. A., and Meyer, M. R. 2005. *Astrophys. J., 622*, 404-429.

Kessler, J. E., Blake, G. A., and Qi, C. 2003. in *Chemistry as a Diagnostic of Star Formation* (C. L. Curry and M.Fich, eds), NRC Press, Ottawa, Canada, 2003, p. 188. 188.

Kitamura, Y., M. Momose, S. Yokogawa, R. Kawabe et al. 2002. *Astrophys. J., 581*, 357-380.

Klahr, H. H. and Bodenheimer, P. 2003. *Astrophys. J., 582*, 869-892.

Koerner, D.M., Sargent, A.I., and Beckwith, S.V.W. 1993. *Icarus, 106*, 2-12.

Lada, C. J. and Lada, E. A. 2003. *Ann. Rev. Astron. Astrophys., 41*, 57-115.

Lahuis, F., et al. 2006. *Astrophys. J., 636*, L145-148.

Larsson, M., Danared, H., Larson, Å., Le Padellec, A., Peterson, J.R. et. al. 1997. *Phys. Rev. Let., 79*, 395-398.

Léger, A., Jura, M., and Omont, A. 1985. *Astron. Astrophys., 144*, 147-160.

Le Teuff, Y. H., Millar, T. J., and Markwick, A. J. 2000. *Astron. Astrophys. Suppl., 146*, 157-168.

Lewis, J. S. and Prinn, R. G. 1980. *Astrophys. J., 238*, 357-364.

Li, A. and Lunine, J. I. 2003. *Astrophys. J., 594*, 987-1010.

MacPherson, G. J., Wark, D. A., and Armstrong, J. T. 1988. In *Meteorites and the Early Solar System*, 746-807.

Malfait, K., Waelkens, C., Waters, L. B. F. M., Vandenbussche, B.

et. al. 1998. *Astron. Astrophys., 332*, L25-L28.

Maloney, P. R., Hollenbach, D. J., and Tielens, A. G. G. M. 1996. *Astrophys. J., 466*, 561.

Markwick, A. J., Ilgner, M., Millar, T. J., and Henning, T. 2002. *Astron. Astrophys., 385*, 632-646.

McCall, B. J., and 15 colleagues 2004. *Phys. Rev. A, 70*, 052716.

Meier, R., Owen, T. C., Jewitt, D. C., Matthews, H. E. et al. 1998. *Science, 279*, 1707.

Millar, T. J., Bennett, A., and Herbst, E. 1989. *Astrophys. J., 340*, 906-920.

Morrison, R. and McCammon, D. 1983. *Astrophys. J., 270*, 119-122.

Mumma, M. J., Weissman, P. R., and Stern, S. A. (1993) In *Protostars and Planets III*, (E. Levy and J. Lunine, eds.), pp. 1177-1252. Univ. of Arizona, Tucson.

Najita, J., Carr, J. S., and Mathieu, R. D. 2003. *Astrophys. J., 589*, 931-952.

Najita, J., Bergin, E. A., and Ullom, J. N. 2001. *Astrophys. J., 561*, 880-889.

Nakagawa, Y., Nakazawa, K., and Hayashi, C. 1981. *Icarus, 45*, 517-528.

Nishi, R., Nakano, T., and Umebayashi, T. 1991. *Astrophys. J., 368*, 181-194.

Nomura, H. 2002. *Astrophys. J., 567*, 587-595.

Nomura, H. and T. J. Millar 2005. *Astron. Astrophys, 438*, 923-938.

Parise, B., and 14 colleagues 2005. *Astron. Astrophys., 431*, 547-554.

Parise, B., Castets, A., Herbst, E., Caux, E., Ceccarelli, C. et. al. 2004. *Astron. Astrophys., 416*, 159-163.

Parise, B., Ceccarelli, C., Tielens, A. G. G. M., Herbst, E. et. al. 2002. *Astron. Astrophys., 393*, L49-L53.

Pontoppidan, K. M., Dullemond, C. P., van Dishoeck, E. F., Blake, G. A. et. al. 2005. *Astrophys. J., 622*, 463-481.

Pringle, J. E. 1981. *Ann. Rev. Astron. Astrophy., 19*, 137-162.

Prinn, R. G. (1993) In *Protostars and Planets III*, (E. Levy and J. Lunine, eds.), pp. 1005-1028. Univ. of Arizona, Tucson.

Prinn, R. G. 1990. *Astrophys. J., 348*, 725-729.

Prinn, R. G. and Fegley, B. 1981. *Astrophys. J., 249*, 308-317.

Przygodda, F., van Boekel, R., Àbrahàm, P., Melnikov, S. Y. et. al. 2003. *Astron. Astrophys., 412*, L43-L46.

Qi., C. et al. 2004. *Astrophys. J., 616*, L7-10.

Qi, C., Kessler, J. E., Koerner, D. W., Sargent, A. I., and Blake, G. A. 2003. *Astrophys. J., 597*, 986-997.

Richter, M. J., Jaffe, D. T., Blake, G. A., and Lacy, J. H. 2002. *Astrophys. J., 572*, L161-L164.

Roberts, H., Herbst, E., and Millar, T. J. 2004. *Astron. Astrophys., 424*, 905-917.

Roberts, H., Fuller, G. A., Millar, T. J., Hatchell, J., and Buckle, J. V. 2002. *Astron. Astrophys., 381*, 1026-1038.

Rodriguez-Franco, A., Martín-Pintado, J., and Fuente, A. 1998. *Astron. Astrophys., 329*, 1097-1110.

Roueff, E., Lis, D. C., van der Tak, F. F. S., Gerin, M., and Goldsmith, P. F. 2005. *Astron. Astrophys., 438*, 585-598.

Sako, S., Yamashita, T., Kataza, H., Miyata, T. et al. T. 2005. *Astrophys. J., 620*, 347-354.

Sano, T., Miyama, S. M., Umebayashi, T., and Nakano, T. 2000. *Astrophys. J., 543*, 486-501.

Schutte, W. A. and Khanna, R. K. 2003. *Astron. Astrophys., 398*, 1049-1062.

Semenov, D., Wiebe, D., and Henning, T. 2004. *Astron. Astrophys., 417*, 93-106.

Shakura, N. I. and Sunyaev, R. A. 1973. *Astron. Astrophys., 24*, 337-355.

Shen, C. J., Greenberg, J. M., Schutte, W. A., and van Dishoeck, E. F. 2004. *Astron. Astrophs., 415*, 203-215.

Simon, M., Dutrey, A., and Guilloteau, S. 2000. *Astrophys. J., 545*, 1034-1043.

Stäuber, P., Doty, S. D., van Dishoeck, E. F., and Benz, A. O. 2005. *Astron. Astrophys., 440*, 949-966.

Stevenson, D. J. 1990. *Astrophys. J., 348*, 730-737.

Stone, J. M., Gammie, C. F., Balbus, S. A., and Hawley, J. F. 2000. In *Protostars and Planets IV*, (V. Mannings et al., eds.), Univ. of Arizona, Tucson, 589.

Störzer, H. and Hollenbach, D. 1998. *Astrophys. J., 502*, L71.

Thi, W.-F., van Zadelhoff, G.-J., and van Dishoeck, E. F. 2004. *Astron. Astrophys., 425*, 955-972.

Thi, W. F., Pontoppidan, K. M., van Dishoeck, E. F., Dartois, E., and d'Hendecourt, L. 2002. *Astron. Astrophys., 394*, L27-L30.

Thi, W. F., and 10 colleagues 2001. *Astrophys. J., 561*, 1074-1094.

Tiné, S., Roueff, E., Falgarone, E., Gerin, M., and Pineau des Forêts, G. 2000. *Astron. Astrophys., 356*, 1039-1049.

Turner, N.J., Willacy, K., Bryden, G., and Yorke, H.W. 2006. *Astrophys. J.*, in press.

Uchida, K. I., and 19 colleagues 2004. *Astrophys. J. Suppl., 154*, 439-442.

Umebayashi, T. and Nakano, T. 1981. *Pub. Astron. Soc. Japan, 33*, 617.

van Boekel, R., Min, M., Waters, L. B. F. M., de Koter, A. et al. 2005. *Astron. Astrophys., 437*, 189-208.

van Dishoeck, E. F. 2004. *Ann. Rev. Astron. Astrophys., 42*, 119-167.

van Dishoeck, E. F., Thi, W.-F., and van Zadelhoff, G.-J. 2003. *Astron. Astrophys., 400*, L1-L4.

van Dishoeck, E. F., Blake, G. A., Draine, B. T., and Lunine, J. I. (1993) In *Protostars and Planets III*, (E. Levy and J. Lunine, eds.), pp. 163-241. Univ. of Arizona, Tucson.

van Dishoeck, E. F. and Dalgarno, A. 1984. *Icarus, 59*, 305-313.

van Dishoeck, E. F., Jonkheid, B., and van Hemert, M.C. 2006. *Faraday Discussions, 133*, in press.

van Zadelhoff, G.J., van Dishoeck, E.F., Thi, W.F., and Blake, G.A. 2001. *Astron. Astrophys., 377*, 566-580.

van Zadelhoff, G.-J., Aikawa, Y., Hogerheijde, M. R., and van Dishoeck, E. F. 2003. *Astron. Astrophys., 397*, 789-802.

Walmsley, C. M., Flower, D. R., and Pineau des Forêts, G. 2004. *Astron. Astrophys., 418*, 1035-1043.

Watson, D. M., and 20 colleagues 2004. *Astrophys. J. Suppl., 154*, 391-395.

Weidenschilling, S. J. 1997. *Icarus, 127*, 290-306.

Weidenschilling, S. J. and Cuzzi, J. N. 1993. In *Protostars and Planets III*, (E. Levy and J. Lunine, eds.), Univ. of Arizona, Tucson, 1031-1060.

Weingartner, J. C. and Draine, B. T. 2001. *Astrophys. J., 563*, 842-852.

Wehrstedt, M. and Gail, H.-P. 2003. *Astron. Astrophys., 410*, 917-935.

Westley, M. S., Baragiola, R. A., Johnson, R. E., and Baratta, G. A. 1995. *Nature, 373*, 405.

Willacy, K., Langer, W. D., and Allen, M. 2006. *Astrophys. J.*, in press.

Willacy, K. and Langer, W. D. 2000. *Astrophys. J., 544*, 903-920.

Willacy, K., Klahr, H. H., Millar, T. J., and Henning, T. 1998. *Astron. Astrophys., 338*, 995-1005.